Non-covalent proteasome inhibitor PI-1840 induces apoptosis and autophagy in osteosarcoma cells

YUXI CHEN[1], HONGJUN CHEN[1], HUI XIE[2], SHAOHUI YUAN[1], CHUANBO GAO[3], LEI YU[1] and ZHENGGANG BI[1]

[1]Department of Orthopedic Surgery, The First Affiliated Hospital of Harbin Medical University, Harbin, Heilongjiang 150001; [2]Teaching Experiment Center of Biotechnology, Harbin Medical University, Harbin, Heilongjiang 150086; [3]Department of Orthopedic Surgery, The Fifth Hospital of Harbin, Heilongjiang 150001, P.R. China

Received September 13, 2018; Accepted February 22, 2019

DOI: 10.3892/or.2019.7040

Abstract. Osteosarcoma (OS) is the predominant form of primary bone malignancy in children and adolescents. Although the combination of chemotherapy and modified surgical therapy leads to marked improvements in the survival rate, the therapeutic outcomes remain unsatisfactory. Therefore, the identification of novel drugs with higher efficacy and fewer side-effects is urgently required. Proteasome inhibitors have been approved by the Food and Drug Administration (FDA) for the treatment of certain cancers, although none of them are directed against OS. Non-covalent proteasome inhibitors, such as PI-1840, are superior to covalent ones in numerous respects in view of their chemical structure; however, to date, no studies have been published on the effects of non-covalent proteasome inhibitors on OS cells. In the present study, the antineoplastic effects of PI-1840 were systematically evaluated in the OS cell lines, MG-63 and U2-OS. Cell viability and morphological changes were assessed by Cell Counting Kit-8 (CCK-8) and live/dead assays. The cell cycle was analyzed using flow cytometry (FCM) and western blot analysis (assessing the levels of the proteins p21, p27, and the tyrosine kinase, WEE1). The extent of cell apoptosis and autophagy were assessed by FCM, western blot analysis [of the apoptosis-associated proteins, microtubule-associated protein 1 light chain 3 α (LC3) and Beclin1], and mRFP-GFP-LC3 adenovirus transfection assay. Transwell and wound healing assays, and western blot analysis of the matrix metalloproteinases (MMPs)2 and 9 were performed to preliminarily evaluate the migration and invasion capability of the cells. In the present study, our results revealed that PI-1840 inhibited the proliferation of OS cells and induced apoptosis, partly due to attenuation of the nuclear factor-κB (NF-κB) pathway. In addition, PI-1840-induced autophagy was detected, and inhibiting the autophagy of the OS cells led to an increase in the survival rate of the U2-OS cells rather than of the MG-63 cells. Furthermore, PI-1840 attenuated the migration and invasion capabilities of the OS cells. In conclusion, the present study revealed PI-1840 to be a promising drug for the treatment of OS.

Correspondence to: Professor Zhenggang Bi, Department of Orthopedic Surgery, The First Affiliated Hospital of Harbin Medical University, 23rd Youzheng Street, Harbin, Heilongjiang 150001, P.R. China
E-mail: drbzg1958@yeah.net

Key words: non-covalent proteasome inhibitor, PI-1840, proliferation, cell cycle arrest, apoptosis, autophagy, metastasis, osteosarcoma

Introduction

Osteosarcoma (OS) is one of the commonest malignant solid tumors in children and adolescents, which exhibits a predilection to occur in the metaphysis of long bones, and most commonly occurs in the distal femur (43%), proximal tibia (23%), or humerus (10%) (1). Treatment for the disease is multimodal, incorporating surgery and chemotherapy (2). Among the various treatment strategies, chemotherapy is the most important in view of its multifunctionality, including reduction of the tumor size pre- or post-operation, and inhibition of distant metastases, also preventing their recurrence. Furthermore, large cooperative group studies and international collaborative efforts have demonstrated that the combination of high-dose methotrexate, doxorubicin, and cisplatin (MAP) provides the most effective regimen (3). However, the various drawbacks of chemotherapy, namely, metastasis, recurrence, side-effects induced by the anticancer drugs, and chemoresistance, have yet to be satisfactorily resolved (4). Although ~30 years have passed since key anticancer drugs were introduced, the development of novel therapeutic drugs for OS has stagnated (5). Therefore, the development of novel drugs and treatments with higher efficacies and fewer side-effects is urgently required.

Protein homeostasis, which serves an important role in maintaining normal cellular metabolism, is precisely regulated according to complex processes. Proteasomes have a critical role in regulating this process. Although essential for normal cell regulation, proteasomal activity, in particular, is pivotal for the proliferation of cancer cells. It has been reported that the level and activity of proteasomes are >90% higher in primary tumors compared with normal tissues (6), and it is widely accepted that high levels of proteasomal activity

provide survival benefits for tumor cells in continuous proliferation (7,8). In recent years, emerging evidence has suggested that proteasome inhibitors may contribute towards promising anticancer strategies (9), and a large number of them have been used in clinical practice (10-12). However, only a few of these proteasome inhibitors have been demonstrated to inhibit the growth of OS cells (13,14); furthermore, none of them have been approved by the Food and Drug Administration (FDA) for the treatment of OS due to the high therapeutic doses required and serious side-effects. Additionally, all of them are covalent, and covalent inhibitors have highly reactive and unstable chemical groups, which render them less suitable as inhibitors (15). PI-1840, which is a novel non-covalent proteasome inhibitor, was first synthesized and reported in 2013 (16). Subsequently, it was revealed that PI-1840 was able to inhibit the growth of several types of tumor cells, and to act non-covalently. In addition, PI-1840 was revealed to be more active against solid tumors (17); however, few systematic studies have been published on the effects of non-covalent proteasome inhibitors on OS cells. In the present study, two cell lines, MG-63 and U2-OS, were selected to investigate the possible molecular mechanisms involved in the antitumor effects of PI-1840 *in vitro*. It was revealed that PI-1840 functioned well in the two cell lines owing to its antitumor effects, including inhibition of growth and metastasis, as well as inducing cell cycle arrest and increasing the levels of apoptosis and autophagy. Collectively, these findings indicated that PI-1840 may be a promising anticancer agent against OS.

Materials and methods

Reagents and antibodies. PI-1840 was purchased from Selleck Chemicals (Houston, TX, USA). HyClone™ Dulbecco's modified Eagle's medium (DMEM) was purchased from GE Healthcare (Chicago, IL, USA). McCoy's 5A medium was purchased from Wuhan Boster Biological Technology, Ltd., Wuhan, China). Fetal bovine serum (FBS) was purchased from Roya Bio-Technology Co., Ltd. (Lanzhou, China). Dimethyl sulfoxide (DMSO) and the Cell Counting Kit-8 (CCK-8) assay were obtained from MedChem Express (Monmouth Junction, NJ, USA). The Invitrogen® LIVE/DEAD® Viability/Cytotoxicity Assay kit was purchased from Thermo Fisher Scientific, Inc. (Waltham, MA, USA). The Annexin V-Fluorescein Isothiocyanate (FITC) Apoptosis Detection and Cell Cycle and Apoptosis Analysis kits (C1062 and C1052, respectively) were acquired from Beyotime Institute of Biotechnology (Shanghai, China). Antibodies against p21 (dilution 1:500; cat. no. WL0362), p27 (dilution 1:500; cat. no. WL01769), Bax (dilution 1:1,000; cat. no. WL01637), B-cell lymphoma-2 (Bcl-2) (dilution 1:500; cat. no. WL01556), caspase-8 (dilution 1:500; cat. no. WL02434), cleaved caspase-8 (dilution 1:500; cat. no. WL0153), cleaved poly ADP-ribose polymerase (PARP) (dilution 1:500; cat. no. WL01932), cytochrome *c* (Cyto *c*) (dilution 1:500; cat. no. WL01571), Beclin1 (dilution 1:500; cat. no. WL02508), microtubule-associated protein light chain 3 (LC3) II/I (Ic3α/β; dilution 1:500; cat. no. WL01506), matrix metalloproteinase 2 (MMP2) (dilution 1:500; cat. no. WL1579), MMP9 (dilution 1:500; cat. no. WL01580), β-actin (dilution 1:1,000; cat. no. WL01845) and cytochrome *c* oxidase (COX IV) (dilution 1:1,000; cat. no. WL02203) were all obtained from Wanleibio Co., Ltd. (Shenyang, China). Antibodies against GAPDH (dilution 1:1,000; cat. no. 5174), β-tubulin (dilution 1:1,000; cat. no. 2146), phosphorylated (p)-p65 (dilution 1:1,000; cat. no. 8242), p65 (dilution 1:1,000; cat. no. 3033), IκBα (dilution 1:1,000; cat. no. 4812), p-IκBα (dilution 1:1,000; cat. no. 2859), and the tyrosine kinase, WEE1 (dilution 1:1,000; cat. no. 4936), were purchased from Cell Signaling Technology, Inc. (Danvers, MA, USA). The antibody against cleaved caspase-9 (dilution 1:500; cat. no. ab2324) and caspase-9 (dilution 1:500; cat. no. ab2013) were obtained from Abcam (Cambridge, MA, USA). Transwell chambers were obtained from Corning, Incorporated (Corning, NY, USA). SignalSilence® IκBα siRNA I (cat. no. 6327) and SignalSilence® Control siRNA (unconjugated; cat. no. 6568) were obtained from Cell Signaling Technology, Inc. The mRFP-GFP-LC3 adenovirus (cat. no. HB-AP2100001) was purchased from HanBio Biotechnology Co. Ltd. (Shanghai, China). z-VAD-fmk and chloroquine (Selleck Chemicals) were kindly provided by Dr Zou Jilong (Department of Orthopedic Surgery, The First Affiliated Hospital of Harbin Medical University, Harbin, China). All other reagents and experimental materials were purchased from common commercial sources.

Cell culture and treatment. The MG-63 and U2-OS OS cell lines were purchased from the Type Culture Collection of the Chinese Academy of Sciences, Shanghai Institute of Cell Biology (Shanghai, China). The MG-63 and U2-OS cells were separately cultured in DMEM or McCoy's 5A medium with 10% FBS and 1% penicillin/streptomycin antibiotics. All the cells were maintained at 37˚C in a humidified atmosphere of 95% air and 5% CO_2. The cells were treated with indicated concentrations of PI-1840 and DMSO (vehicle used as a control; the concentration of DMSO was <0.1%, which would not have affected the physiological status of the OS cells). The concentration of the stock solution of PI-1840 used was 40 mM (in DMSO).

Observation of morphological changes. The MG-63 and U2-OS cells were seeded into 6-well plates at a density of $1x10^6$ cells/well, and subsequently allowed to attach to the wells at 37˚C for 12 h. The cultures were then treated with the different concentrations of PI-1840 (MG-63: 0, 30 and 60 μM; U2-OS: 0, 20 and 40 μM), and incubated at 37˚C for 48 h. Morphology of the cells was then observed under an inverted microscope (Olympus Corp., Tokyo, Japan), and images were captured at a magnification of x100.

Cell viability assay. The inhibitory effects of PI-1840 on the OS cells were evaluated using CCK-8 assays. A cell suspension was produced from OS cells, and the cells were counted. Subsequently, the cells were seeded into a 96-well plate at a density of $5x10^3$ cells/well, and incubated for 12 h to allow attachment of the cells to take place. The cells were then treated with various concentrations of PI-1840 (0, 5, 10, 20, 40, 80 and 160 μM) for 24 or 48 h. CCK-8 solution was mixed with serum-free medium at a concentration of 10%, and subsequently replaced with the former medium without any bubbles during the procedure. The plate was then incubated for 1-4 h in the incubator at 37˚C. Finally, the absorbance was

measured at 450 nm using a microplate reader (BioTek China, Beijing, China).

Live/dead viability/cytotoxicity assay. This assay was performed using a LIVE/DEAD® Viability/Cytotoxicity Assay kit (Thermo Fisher Scientific, Inc.). Following the manufacturer's protocol, MG-63 and U2-OS cells were separately suspended and seeded into 6-well plates at a density of $1x10^6$/well, after having incubated the cells at 37˚C for 12 h to allow them to adhere to the plate. The cells were subsequently treated with different concentrations of PI-1840 (MG-63: 0, 30 and 60 μM; U2-OS: 0, 20 and 40 μM) for 48 h at 37˚C. At the end of this incubation period, the cells were washed twice with phosphate-buffered saline (PBS) and incubated for a further 15 min at 37˚C; during this procedure, the cells were incubated with DMEM or McCoy's 5A solution containing 2.5 μM Calcein AM and 4 μM ethidium homodimer-1 in the dark. Finally, the live and the dead cells (determined from the green or the red fluorescence, respectively) were observed and counted with a fluorescence microscope (Olympus Corp.).

Cell cycle analysis. OS cells were seeded into 6-well plates at a density of $1x10^6$ cells/well, and subsequently incubated for 12 h at 37˚C. After attachment, MG-63 and U2-OS cells were separately treated with PI-1840 (MG-63, 60 μM; U2-OS, 40 μM) for 24 or 48 h at 37˚C. The cells were harvested after centrifugation (1,000 x g for 5 min), and washed with PBS twice. Subsequently, the cells were fixed with 70% ethanol at 37˚C overnight, centrifuged (1,000 x g for 5 min) and washed again; the supernatant was subsequently discarded. Staining buffer (500 μl) was added to each sample, and then the samples were slowly resuspended. Propidium iodide (PI) (25 μl) and ribonuclease (RNase) A (10 μl) were added into each sample. Avoiding light, the samples were incubated for 30 min at 37˚C, and subsequently stored on ice. All the samples were analyzed using a flow cytometer (Becton, Dickinson and Company, Franklin Lakes, NJ, USA).

Cell apoptosis analysis. The apoptotic effects of PI-1840 on MG-63 and U2-OS cells were evaluated using the Annexin V-FITC/PI double staining assay (Beyotime Institute of Biotechnology). Briefly, OS cells were seeded into 6-well plates at a density of $1x10^6$ cells/well, and subsequently incubated for 12 h at 37˚C to allow adherence to take place. Next, cells were treated with different concentrations (MG-63: 0, 15, 30 and 60 μM; U2-OS: 0, 10, 20 and 40 μM) of PI-1840 for 48 h in an incubator at 37˚C. Following the PI-1840 treatment, cells in each group were harvested and centrifuged for 5 min at 1,000 x g at room temperature. The supernatant was discarded, and subsequently 195 μl Annexin V-FITC binding solution was added to each sample to resuspend the cells. Cells were then stained with 5 μl Annexin V-FITC and 5 μl PI, following the manufacturer's protocol. Subsequently, the samples were incubated for 15 min in the dark. Finally, the samples were analyzed using a flow cytometer (Becton, Dickinson and Company).

Transwell assay. Matrigel™ (BD Biosciences, San Jose, CA, USA) was diluted with cold, filtered distilled water, and subsequently was applied to the upper chamber of the polycarbonate Transwell filters (Corning, Inc.). OS cells were seeded into 6-well plates at a density of $1x10^6$ cells/well, and incubated for 12 h at 37˚C to allow adherence to take place. Subsequently, cells were treated with PI-1840 at the concentration giving rise to half-maximal inhibition (MG-63, 60 μM; U2-OS, 40 μM) for 48 h. Cells were digested using trypsin, and then were resuspended and counted. Cell suspension (200 μl) was added into the upper chamber at a density of $2x10^4$ cells/well, and subsequently 800 μl medium containing 30% FBS was added into the lower chamber of each well of the 24-well plates. Cells were subsequently incubated for 48 h. The Transwell filters were washed with PBS twice, and cells were fixed at room temperature using 4% paraformaldehyde (Sigma-Aldrich; Merck KGaA, Darmstadt, Germany) for 15 min. After drying, cells were stained using 0.5% crystal violet (Amresco, LLC, Solon, OH, USA) for 5 min, and subsequently rinsed with distilled water. Finally, images were captured at a magnification of x200 by an inverted microscope (Motic, AE31; Motic Incorporation, Ltd., Causeway Bay, Hong Kong), and the cells were counted.

Wound healing assay. OS cells were seeded at a density of $2x10^6$ cells/well in 6-well plates and incubated for 12 h at 37˚C to allow adherence to take place. The cells were wounded using a 10-μl white tip, and subsequently treated with various concentrations of PI-1840 (MG-63: 0, 60 μM; U2-OS: 0, 40 μM). The distances between the two edges were observed using a microscope (Nikon Corp., Tokyo, Japan) at different time-points (0, 12 and 24 h), and the area of closure was assessed using ImageJ (1.46r) software (National Institutes of Health, Bethesda, MD, USA).

Western blotting. OS cells were seeded into 6-well plates at a density of $1x10^6$ cells/well, and incubated for 12 h at 37˚C to allow adherence to take place. Subsequently, the medium was replaced by medium mixed with different amounts of PI-1840 (MG-63: 15, 30 and 60 μM; U2-OS: 10, 20 and 40 μM) or vehicle (DMSO), and the cells were incubated at 37˚C for 24 or 48 h. After incubation with the drug, the cells were washed with PBS three times, and then lysed with cold radioimmunoprecipitation (RIPA) buffer (Wanleibio Co., Ltd., WLA019) containing 1% phenylmethanesulfonyl fluoride and 10% phosphatase inhibitor, after which the cell lysates were sonicated. The supernatants were collected after centrifugation at 12,000 x g for 15 min at 4˚C, and subsequently the protein concentration was measured using a bicinchoninic acid (BCA) protein assay kit (Beyotime Institute of Biotechnology). As far as the mitochondrial proteins were concerned, a cell mitochondria isolation kit (Beyotime Institute of Biotechnology) was used prior to lysing with cold RIPA buffer. The proteins were separated by SDS-PAGE (concentration gel 5%, separation gel 12%), and then transferred to polyvinylidene fluoride membranes. After blocking with 5% non-fat milk for 2 h at room temperature, the membranes were incubated with the primary antibodies (diluted in TBS) of interest overnight at 4˚C (see the *Reagents and antibodies* section aforementioned for full details of the applied antibodies). Then, the membranes were placed into TBST, and shaken for 5 min at room temperature, and this step was repeated four times. Subsequently, the appropriate secondary antibody (goat anti-rabbit IgG-HRP;

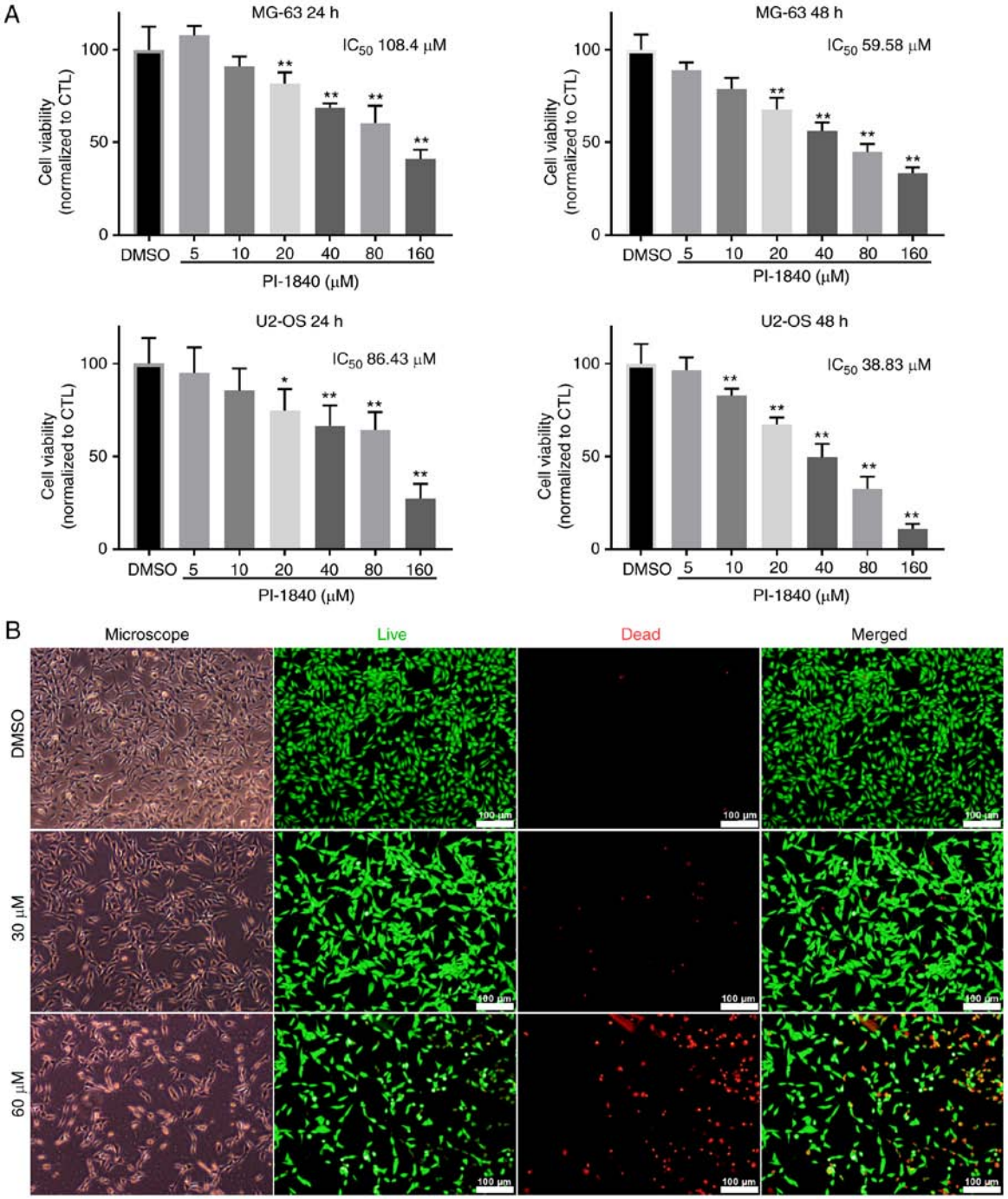

Figure 1. PI-1840 inhibits proliferation of OS cells. (A) PI-1840 dose-dependently reduced the viability of the MG-63 and U2-OS cells after 24 or 48 h treatment (n=10). *P<0.05, **P<0.01 compared with the DMSO group. The IC_{50} values of the OS cells following PI-1840 treatment for 24 or 48 h were calculated using GraphPad Prism software (version 7.0.4). (B) As observed under an inverted microscope (magnification, x100), PI-1840 altered the morphology of the MG-63 cells. PI-1840 significantly reduced the density of live cells (green fluorescence), and increased the number of dead cells (red fluorescence) in a concentration-dependent manner after 48 h treatment; CTL, control; DMSO, dimethyl sulfoxide; OS, osteosarcoma.

dilution 1:5,000; cat. no. WLA023; Wanleibio Co., Ltd.) was added and incubated for 1 h at 37˚C without light, and enhanced chemiluminescence (ECL) substrate (Wanleibio Co., Ltd.) was used to visualize the protein bands. The films were scanned using a WD-9413B Scanner (Beijing Liuyi Culture Co., Ltd, Beijing, China).

Evaluation of fluorescent LC3 puncta. The MG-63 and U2-OS cells were seeded into 24-well plates at a density of $5x10^4$ cells/well and incubated for 12 h at 37˚C. The cells were subsequently transfected with mRFP-GFP-LC3 adenovirus (at a ratio of adenovirus number to cell number of 100:1) for 24 h at 37˚C, according to the manufacturer's protocol, prior to treatment with the various concentrations of PI-1840 (MG-63: 0, 60 μM; U2-OS: 0, 40 μM). Following treatment with PI-1840 for 48 h, the cells were observed under a confocal fluorescence microscope (Olympus Corp.), and images were captured.

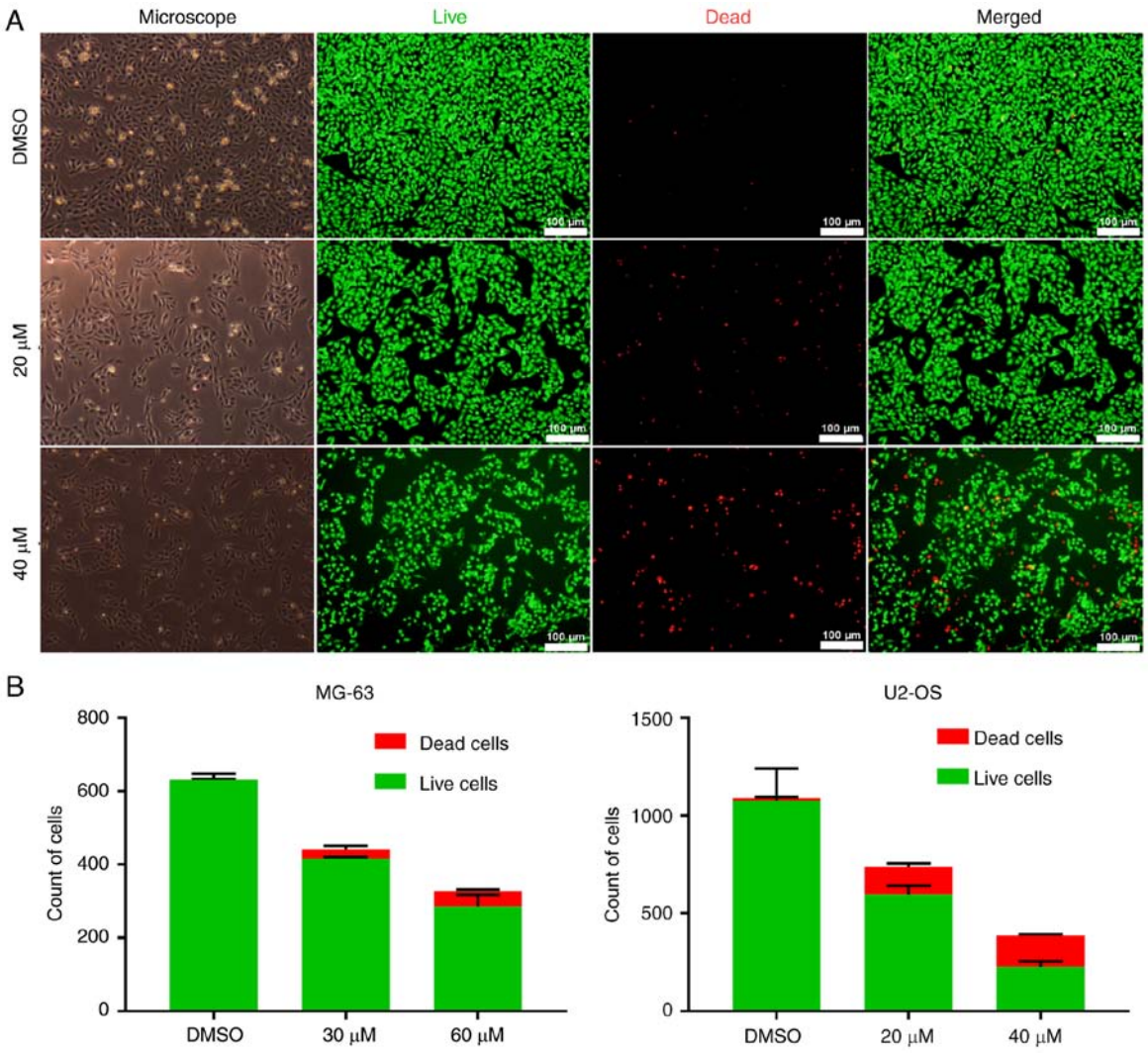

Figure 2. PI-1840 inhibits proliferation of OS cells. (A) As observed under an inverted microscope (magnification, x100), PI-1840 altered the morphology of the U2-OS cells. PI-1840 significantly reduced the density of live cells (green fluorescence), and increased the number of dead cells (red fluorescence) in a concentration-dependent manner after 48 h treatment. (B) Bar chart of the results of live and dead assays (n=4). DMSO, dimethyl sulfoxide; OS, osteosarcoma.

RNA interference knockdown of IκBα. OS cells were seeded into 6-well plates at the density of $5x10^5$/well and incubated for 12 h to allow adherence to take place at the density of 60-70% confluence, and subsequently the cells were transfected with 100 nM IκBα siRNA I or control siRNA with vehicle, and then incubated for 24 h at 37˚C. Subsequently, the cells were treated with or without PI-1840 (MG-63: 0, 60 μM; U2-OS: 0, 40 μM) and incubated at 37˚C for 48 h for subsequent assays. For the transfection procedure, Lipofectamine™ RNAiMAX Transfection reagent (Thermo Fisher Scientific, Inc.) was used, and the manufacturer's protocol was followed.

Statistical analysis. All data values are expressed as the mean ± standard deviation for three or more independent experiments. The IC_{50} values were calculated using GraphPad Prism software, version 7.0.4 (GraphPad Software, Inc., La Jolla, CA, USA). Other statistical analyses were also performed using GraphPad Prism version 7.0.4. Differences were assessed using one-way analysis of variance, followed by Tukey's multiple-comparison test. $P<0.05$ was considered to indicate a statistically significant value.

Results

PI-1840 inhibits the proliferation of MG-63 and U2-OS cells. To assess the effect of PI-1840 on the proliferation of OS cells, a CCK-8 assay was used. As revealed in Fig. 1A, cells were treated with PI-1840 at different concentrations (5-160 μM) for 24 or 48 h. Cell growth was inhibited in a dose-dependent manner following treatment with PI-1840 for 48 h, and the IC_{50} values of the two cell lines at 24 or 48 h were calculated to be 108.40 μM (MG-63, 24 h), 59.58 μM (MG-63, 48 h), 86.43 μM (U2-OS, 24 h), and 38.83 μM (U2-OS, 48 h), respectively. Morphological observation and a LIVE/DEAD® viability/cytotoxicity assay was also employed to confirm the cytotoxicity of PI-1840 on OS cells. As revealed in Figs. 1B and 2A, the cell density and the number of cells with a normal distribution pattern were decreased, and the number of atrophic or floating cells was increased, upon administration of an increasing concentration of PI-1840. As the concentration of the drug was increased, the density of live cells (determined by the green fluorescence) was reduced, whereas the dead cells (shown by the red fluorescence) exhibited the opposite trend (Figs. 1B, and 2A and B).

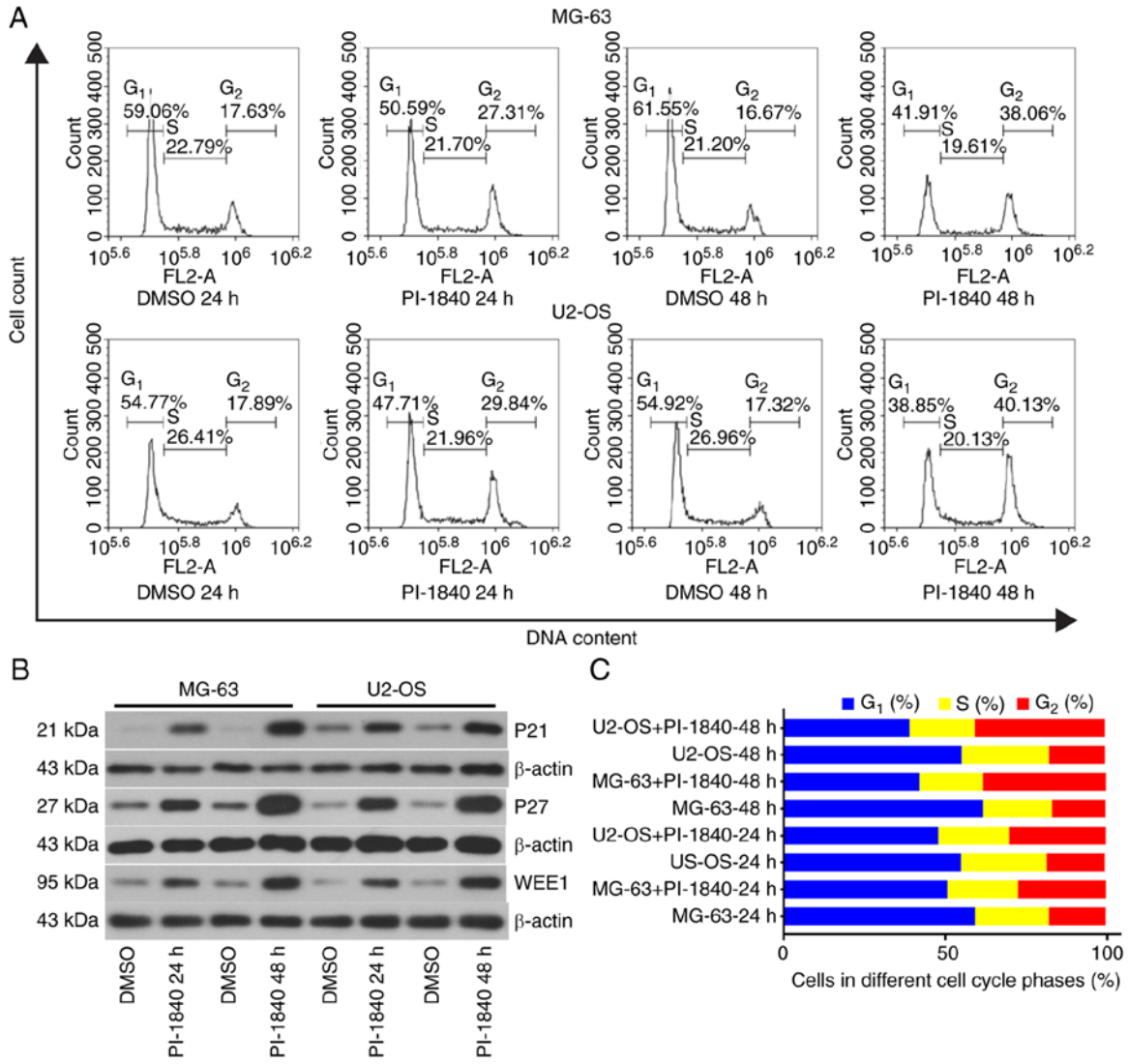

Figure 3. PI-1840 induces cell cycle arrest at the G_2/M phase in OS cells. (A and C) FCM analysis of the cell cycle arrest following treatment with PI-1840 (60 μM for MG-63, and 40 μM for U2-OS) for 24 or 48 h. (B) Western blotting of cell cycle-associated proteins (p21, p27, WEE1). OS, osteosarcoma; FCM, flow cytometry.

PI-1840 induces cell cycle arrest at the G_2/M phase. To determine the mechanism of inhibition of proliferation, cell cycle distributions of the OS cells were analyzed using flow cytometric analysis. As revealed in Fig. 3A and C, a marked increase in the G_2/M phase cell population was observed for the two cell lines after 24 or 48 h treatment of PI-1840 at the indicated concentrations. For further confirmation of cell cycle arrest, western blot assays were also performed. As revealed in Figs. 3B, and 4A and B, the cell cycle regulation-associated proteins, p21, p27 and WEE1, accumulated in a time-dependent manner following treatment with PI-1840 at the indicated time-points.

PI-1840 induces apoptosis in MG-63 and U2-OS cells. To further investigate the death of the OS cells, Annexin V-FITC/PI double staining assay was performed. As revealed in Fig. 5A, LL, LR, UR and UL represent the live cells, early apoptotic cells, late apoptotic cells, and cellular debris, respectively. The apoptotic rates (Fig. 5B) of the two cell lines were increased by PI-1840 treatment in a dose-dependent manner. Subsequently, to investigate the underlying mechanism, IκBα, p-IκBα, p65, p-p65, and apoptosis-associated proteins were analyzed using western blot analysis. As revealed in Fig. 5C-E, following treatment with PI-1840 for 48 h, the ratio of the expression level of (p-IκBα/control)/(IκBα/control) increased, and that of (p-p65/control)/(p65/control) decreased, in a dose-dependent manner, whereas the expression level of IκBα did not change significantly. These results indicated that the NF-κB pathway was inhibited by the administration of PI-1840. In order to further explore the downstream apoptotic pathway, apoptosis-associated proteins (including those of the extrinsic and intrinsic pathways) were analyzed by western blot assay. As revealed in Fig. 6A-F, as the concentration of PI-1840 increased, the expression level of Bcl-2, which helps cells to avoid apoptosis, was decreased in a dose-dependent manner. Furthermore, the expression level of the mitochondrial proteins Cyto *c* was decreased, while the expression levels of Bax, and the ratios of (cleaved caspase-3/caspase-3, cleaved PARP/PARP, cleaved caspase-8/caspase-8 and cleaved

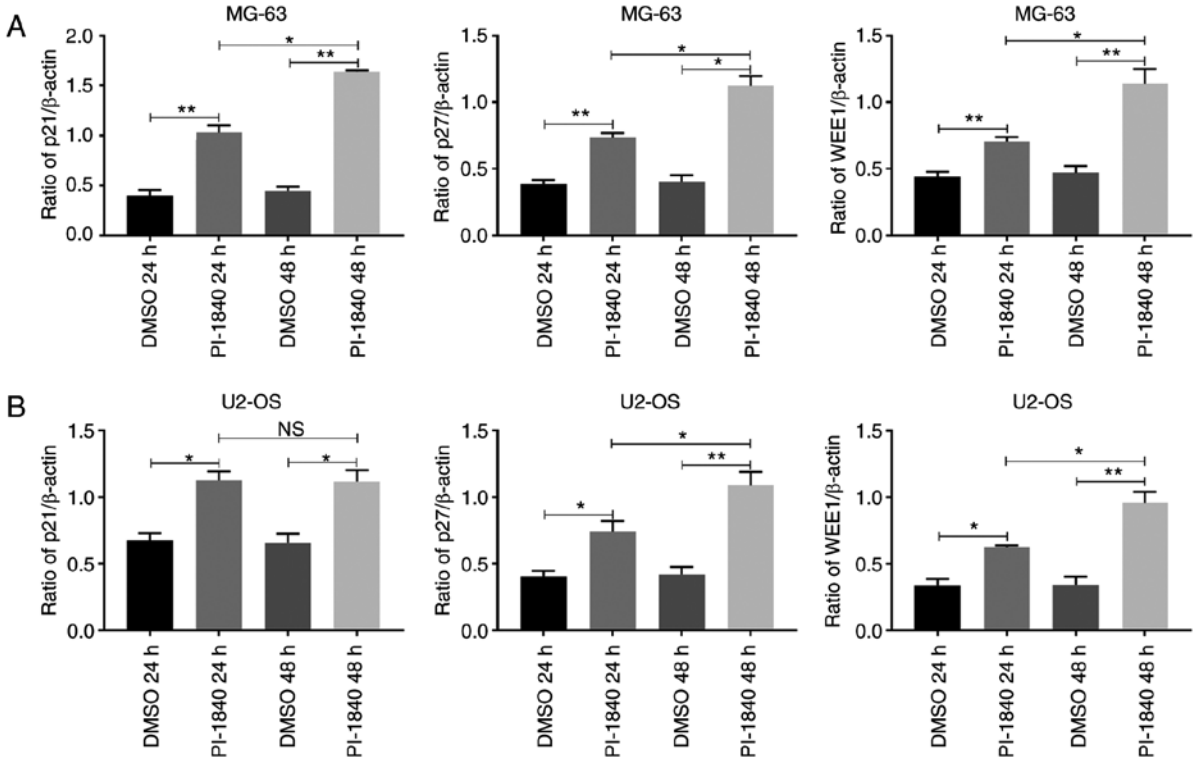

Figure 4. PI-1840 induces cell cycle arrest at the G_2/M phase in OS cells. (A) Western blot statistical analysis of cell cycle-associated proteins (p21, p27, WEE1) of MG-63 cells. (n=3). *P<0.05; **P<0.01 compared with the DMSO group. (B) Western blot statistical analysis of cell cycle-associated proteins (p21, p27, WEE1) of U2-OS cells. (n=3). *P<0.05; **P<0.01 compared with the DMSO group. NS, no significance; OS, osteosarcoma; DMSO, dimethyl sulfoxide.

caspase-9/caspase-9 were increased dose-dependently. The aforementioned results suggested that, in the two cell lines, apoptosis was induced, and the extrinsic and the intrinsic pathways were involved in this process. To evaluate the degree of apoptosis in terms of the reduction of cell viability, pan-caspase inhibitor (z-VAD-fmk) and CCK-8 assays were performed. As revealed in Fig. 7A and B, following co-treatment of the cells with z-VAD-fmk, the percentage of living cells and cell viability were increased significantly, suggesting that PI-1840-induced cell death was caspase-dependent. To explore the association between inhibition of the NF-κB pathway and the execution of apoptosis, SignalSilence® IκBα siRNA I was applied. As revealed in Fig. 7C and D, in the OS cells pretreated with IκBα siRNA and subsequently treated with PI-1840, the PI-1840-induced downregulation of cell viability was attenuated compared with the cells co-treated with SignalSilence® control siRNA and PI-1840. However, the cell viability of the group co-treated with IκBα siRNA and PI-1840 remained higher compared with that of the PI-1840 group (co-treated with SignalSilence® control siRNA and PI-1840). In addition, as revealed in Fig. 7E, activation of the NF-κB pathway through inhibition of the expression of IκBα led to lower expression levels of cleaved caspase-3, which indicated that the caspase-dependent apoptosis pathway was attenuated. Fig. 7F showed that SignalSilence® IκBα siRNA I successfully suppressed the expression of IκBα in both of the two cell lines. Collectively, these results demonstrated that PI-1840 induced caspase-dependent apoptosis, and that this phenomenon may be attributed, at least in part, to the inhibition of NF-κB pathway.

PI-1840 induces autophagy in MG-63 and U2-OS cells. Previous research has shown that autophagy may affect the survival of tumor cells. After having been treated with proteasome inhibitors, the balance of protein metabolism is disrupted, and this probably induces autophagy. Therefore, in the present study, autophagy-associated proteins were also analyzed using western blotting. As revealed in Fig. 8A-E, with an increasing dose of PI-1840, the ratio of LC3 II to LC 3 I increased, and the expression level of Beclin1 was also enhanced. To confirm the occurrence of autophagic flux, mRFP-GFP-LC3 adenovirus transfection was performed. As revealed in Fig. 8F and G, the number of autophagosomes (denoted by the yellow dots in cells) and autolysosomes (red dots in cells) increased significantly following treatment with PI-1840 for 48 h. Subsequently, CCK-8 assays were performed to assess whether the occurrence of PI-1840-induced autophagy was able to affect the cell viability of the two cell lines. As revealed in Fig. 7A, after the inhibition of autophagy with chloroquine, for the MG-63 cell line, the cell viability was not markedly altered compared with the group treated with PI-1840 alone. However, for the U2-OS cells (Fig. 7B), inhibiting autophagy did lead to an attenuation of the effect of PI-1840-induced proliferation inhibition, which suggested that PI-1840-induced autophagy was detrimental to the U2-OS cells. In Fig. 8H and I, western blotting and fluorescence confocal images showed that CQ could abolish the PI-1840 induced autophagy of the OS cells.

PI-1840 inhibits the ability of migration and invasion of OS cells. To determine the effect of PI-1840 treatment on cell migration, a wound healing assay was employed. As revealed

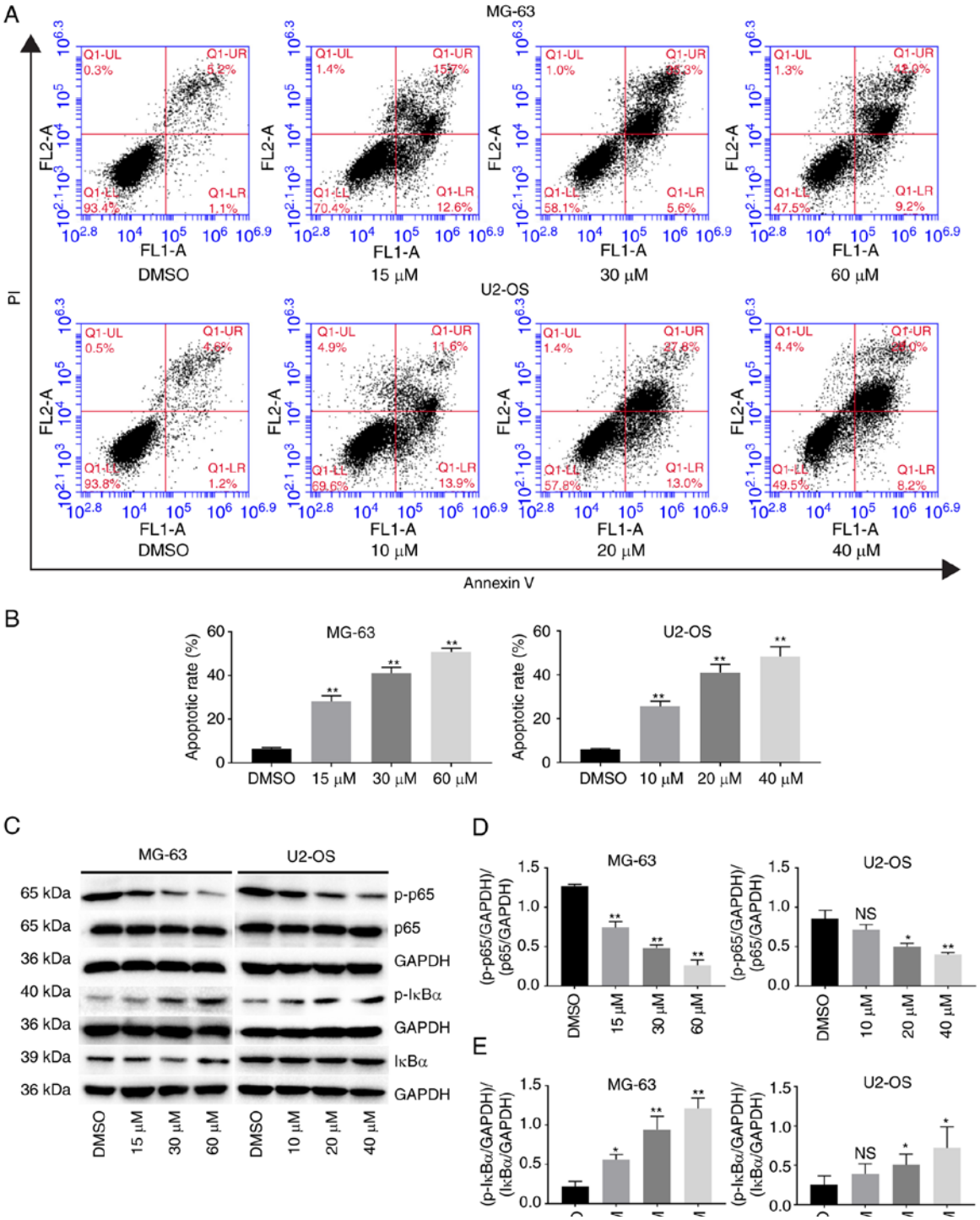

Figure 5. PI-1840 induces the apoptosis of OS cells. (A) PI-1840-induced apoptosis was confirmed using Annexin V-FITC/PI double staining. The cells were exposed to PI-1840 for 48 h at the indicated concentrations. LL, LR, UR, and UL represent live cells, early apoptotic cells, late apoptotic cells, and cellular debris, respectively. (B) Summary plot for the apoptosis rates (apoptosis rates=early apoptotic cell rates + late apoptotic cell rates). (C-E) PI-1840 suppressed the nuclear factor-κB pathway in a dose-dependent manner when cells were exposed to PI-1840 for 48 h at the indicated concentrations (n=3). *P<0.05; **P<0.01 compared with the DMSO group. ns, no significance; OS, osteosarcoma; DMSO, dimethyl sulfoxide.

in Fig. 9A-C, the area between the two edges was markedly decreased following treatment with PI-1840 for 12 and 24 h. To investigate the inhibition of invasion, Transwell assays and western blotting were performed. As revealed in Fig. 10A-C, the number of OS cells decreased significantly in the lower chamber compared with the control group. Furthermore, the expression levels of the investigated MMPs were decreased with an increasing concentration of PI-1840 (Fig. 10E-I). In contrast, after application of IκBα siRNA I, the expression level of MMP2 was increased compared with the group both treated with PI-1840 and control siRNA (Fig. 10D). These findings indicated that PI-1840 was able to interfere with the migration and invasive capabilities of the OS cells via inhibition of the NF-κB pathway.

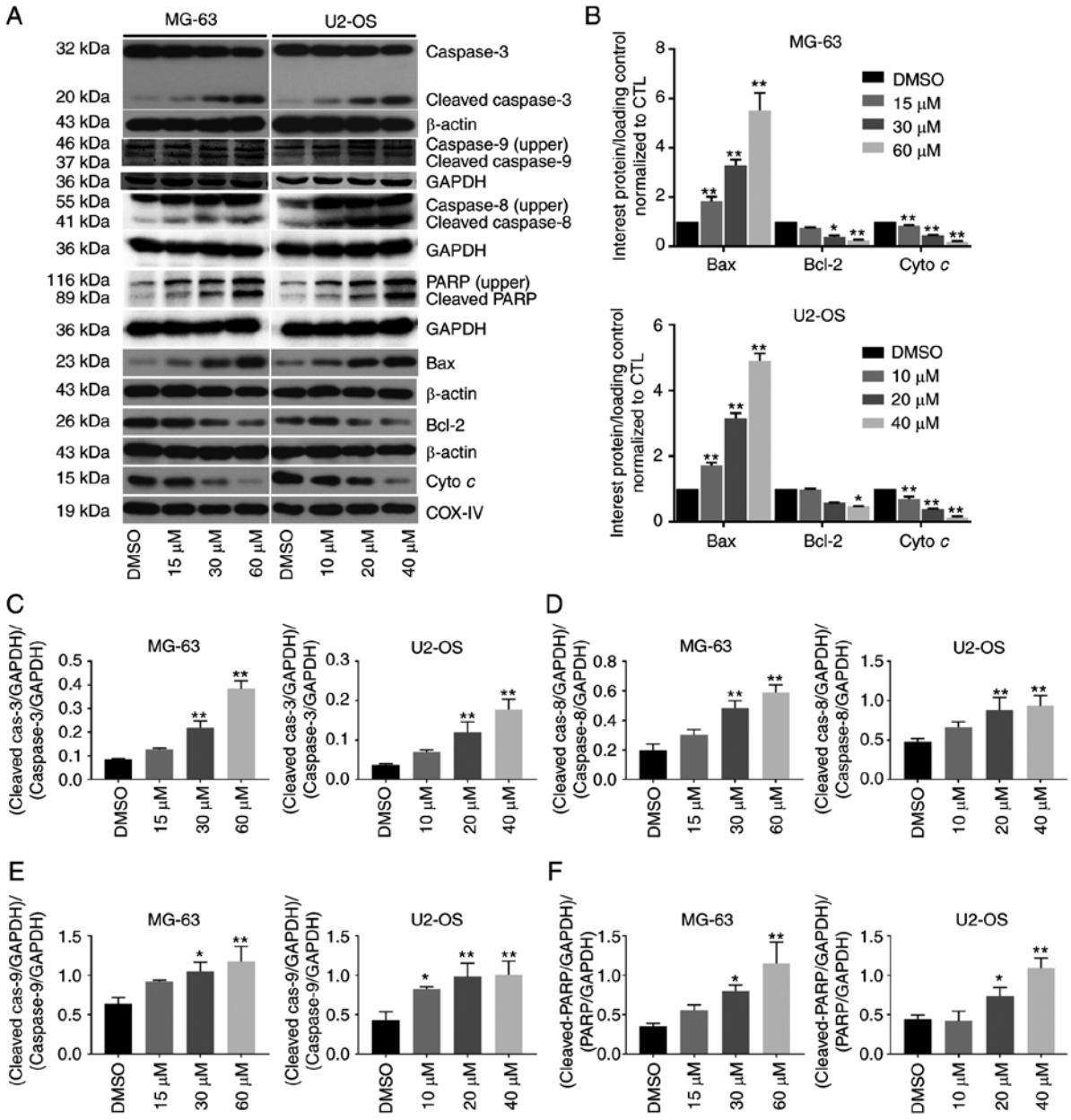

Figure 6. PI-1840 induces the apoptosis of OS cells. (A) Western blot analyses of caspase-3/cleaved caspase-3, caspase-9/cleaved caspase-9, caspase-8/cleaved caspase-8, PARP/cleaved-PARP, Bax, Bcl-2 and Cyto *c*. (B-F) Western blot statistical analysis of caspase-3/cleaved caspase-3, caspase-9/cleaved caspase-9, caspase-8/cleaved caspase-8, PARP/cleaved-PARP, Bax, Bcl-2 and Cyto *c* (exposed to PI-1840 for 48 h; n=3). For caspase-3, -8 and -9 and PARP, the results were presented using '(cleaved-protein/control)/(total protein/control)', *P<0.05; **P<0.01 compared with the DMSO group. ns, no significance; CTL, control; OS, osteosarcoma; DMSO, dimethyl sulfoxide; Bcl-2, B-cell lymphoma-2; Cyto *c*, cytochrome *c*; PARP, poly(ADP-ribose) polymerase.

Discussion

Protein metabolism has a pivotal role in cell function, particularly in tumor cells. The disruption of the protein metabolism process in tumor cells may contribute to catastrophic levels of cell function disorder, affecting the processes of proliferation, apoptosis and metastasis. Protein degradation is predominantly executed through the proteasome (90% of the total) and the lysosome (the remaining 10%). Therefore, targeting the proteasome with proteasome inhibitors provides a promising and feasible approach to suppress cancer. At present, numerous proteasome inhibitors have been developed, and these have continued to draw increasing attention for research purposes. Although bortezomib, carfilzomib, and ixazomib have been approved by the FDA for the treatment of certain types of cancer, the side-effects of these drugs are not negligible. Furthermore, the chemical structure of a large number of already developed proteasome inhibitors, which determines that they bind covalently to the proteasomes, is a major obstacle that hinders them from being applied safely and widely in the clinic. PI-1840 is a novel proteasome inhibitor that has fewer shortcomings compared with the former ones owing to its unique chemical structure. It operates with a non-covalent mode of action, is more selective, and exerts milder effects on normal cells. However, only a small number of systematic studies (17) have been published to date on the anticancer effects and mechanisms of non-covalent proteasome inhibitors, particularly with regard to OS cell lines.

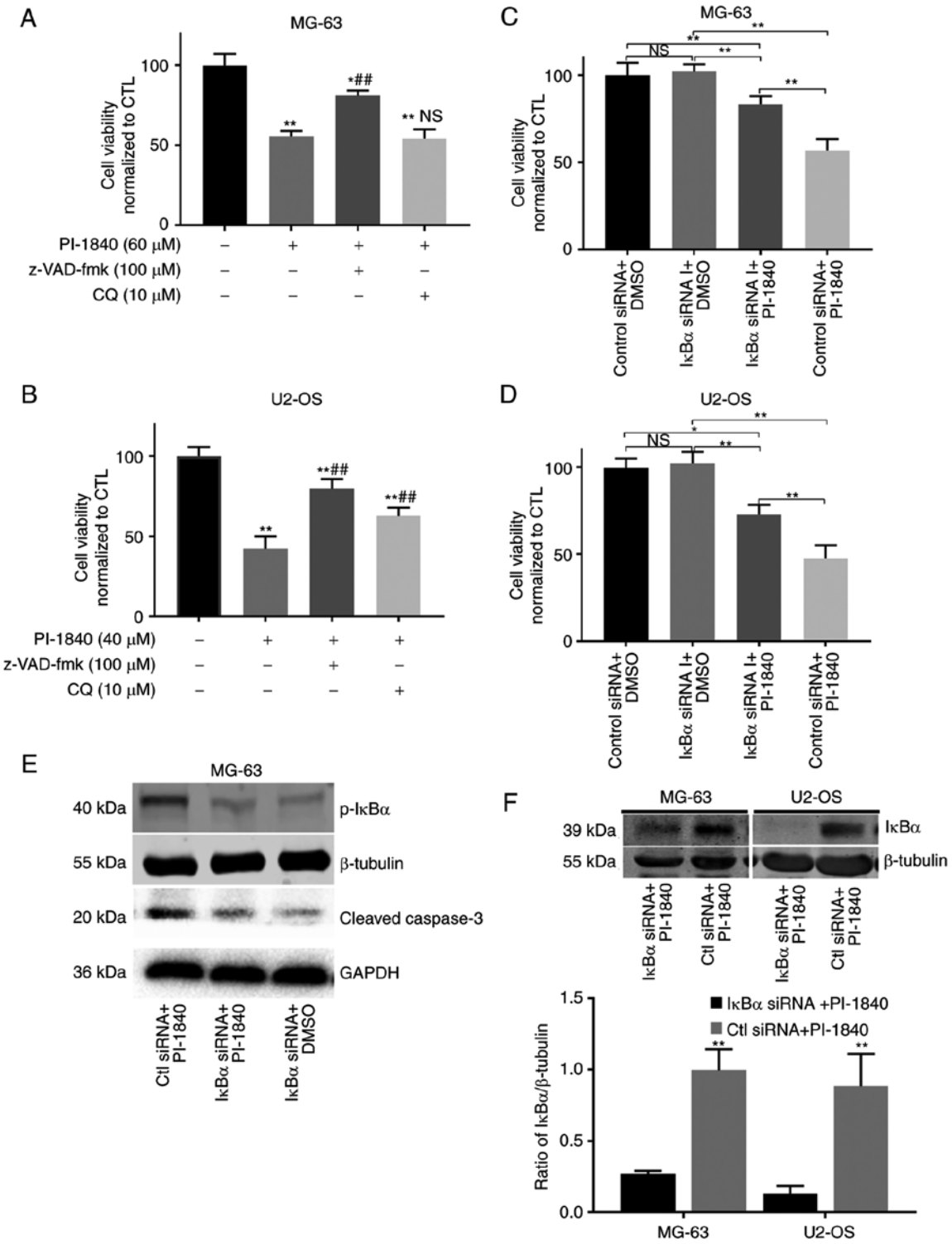

Figure 7. (A and B) With the Cell Counting Kit-8 assays, following treatment with PI-1840 and co-treatment with the pan-caspase inhibitor, z-VAD-fmk, the cell viability increased markedly compared with PI-1840 alone (48 h), although it was still lower compared with that of DMSO group. Concurrently, the results also revealed, following exposure to PI-1840 and co-treatment with CQ (48 h), that the cell viability was not significantly altered in the MG-63 cells, but was increased in the U2-OS cells (n=6). *P<0.05; **P<0.01 compared with the DMSO group; $^{\#\#}$P<0.01 compared with the PI-1840 alone group. (C and D) Blockade of protein IκBα with siRNA increased the cell viability compared with PI-1840 alone (48 h treatment) group. (n=6). *P<0.05; **P<0.01 compared with the control. (E) The expression level of phospho-IκBα was markedly downregulated by siRNA, and cleaved caspase-3 levels decreased subsequently (cells were exposed to the IC50 concentration of PI-1840 for 48 h). (F) The expression of IκBα was suppressed by SignalSilence® IκBα siRNA I (cat. no. 6327) successfully in both of the two cell lines (proteins were obtained after transfection with siRNA for 24 h). (n=3). **P<0.01 compared with the control. CTL, control; DMSO, dimethyl sulfoxide; OS, osteosarcoma; NS, no significance; CQ, chloroquine.

In the present study, the effects of PI-1840 on the OS cell lines, MG-63 and U2-OS, were systematically evaluated, including an assessment of the cell cycle, apoptosis, metastasis and autophagy. Our analyses disclosed that PI-1840 was able to suppress OS cells *in vitro* by various means. To the best of our knowledge, our study is the first to demonstrate: i) That a

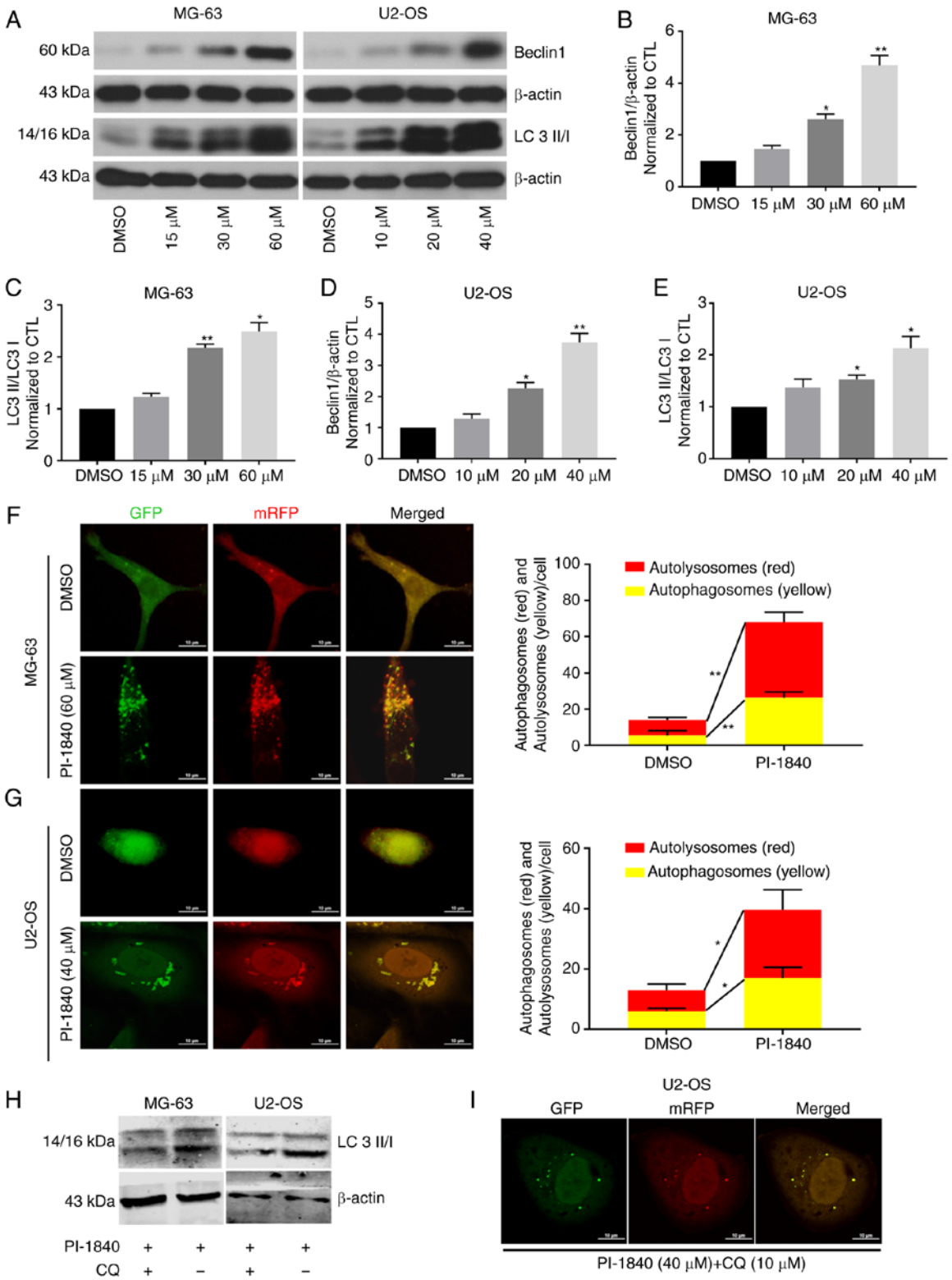

Figure 8. PI-1840 induces autophagy in OS cells. (A-E) The expression level of Beclin1 and the ratio of LC3 II (16 kDa) to LC3 I (14 kDa) were increased with an increasing concentration of PI-1840 (48 h) (n=3). *P<0.05; **P<0.01 compared with the DMSO group. (F and G) PI-1840-induced autophagic flux in OS cells. (OS cells were exposed to the IC50 concentration of PI-1840 for 48 h; n=3). *P<0.05; **P<0.01 compared with the DMSO group. (H and I) Western blotting and mRFP-GFP-LC3 adenovirus were used to examine the inhibition of autophagy resulting from CQ. Autophagy resulting from PI-1840 was abolished by CQ. CTL, control; OS, osteosarcoma; DMSO, dimethyl sulfoxide; CQ, chloroquine.

non-covalent proteasome inhibitor was able to cause the cell cycle arrest of tumor cells; ii) non-covalent proteasome inhibitor-induced autophagy, and its effect on the survival of OS cells; and iii) an inhibition of the invasive capability of OS cell lines.

In the evaluation of the inhibitory effect on proliferation, live/dead viability assays were used. The results revealed that the total number of cells decreased in the treated cells compared with the DMSO cells, which was consistent with

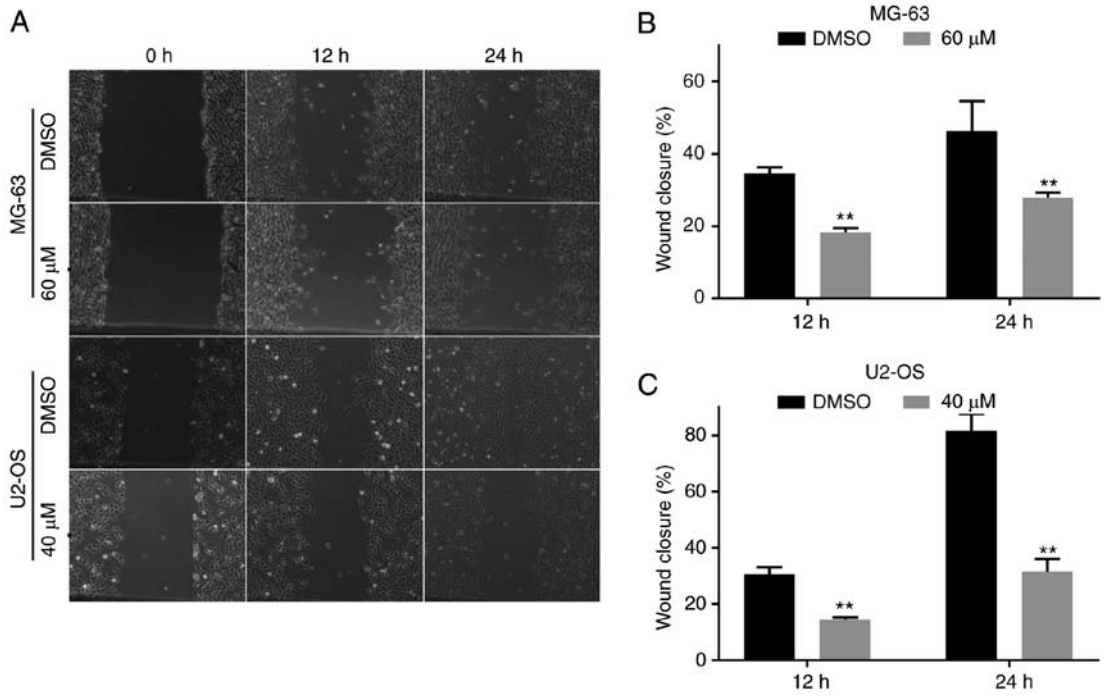

Figure 9. PI-1840 inhibits the migration and invasion abilities of OS cells. (A-C) In the wound healing assay, after treatment with PI-1840 for different time-points, the wound closure area was diminished significantly (magnification, x100; n=3). **P<0.01 compared with the DMSO group. OS, osteosarcoma; DMSO, dimethyl sulfoxide.

our previous study that tested deoxyelephantopin (18). Hereby, we speculated that there are two main reasons which led to the decrease in the total number of cells: Firstly, many dead cells which did not attach to the plate were washed away in the step where the cells were rinsed twice with PBS buffer, while some dead or dying cells still attached to the 6-well plates; and thus, as the concentration of the drug increased, the dead cells increased, and more cells washed away. Thus, the total cells decreased as the concentration of the drug increased. Secondly, since the cells were seeded into the 6-well plates at the same density, after treatment with PI-1840 for 48 h, with the concentration of PI-1840 increasing, the inhibitory effect was stronger, thus the less total number of cells.

A previous study demonstrated that the cell cycle period, and expression levels of cell cycle-associated proteins, may be altered by proteasome inhibitors (19). Therefore, in the present study, the cell cycle period and the cell cycle-associated proteins, p21, p27 and WEE1, were analyzed using flow cytometric analysis and western blotting. p21 and WEE1 are two key cell cycle regulators that block the G_2/M transition by inhibiting the activity of cyclin-dependent kinase 1 (CDK1)/cyclin B (20). It is noteworthy that, in our study, the expression level of p27, which restricts the G_1-S transition by promoting the formation of the CDK2-cyclin E complex to restrain its activity, was also increased. However, the results of the FCM experiments indicated that the G_1-S transition was not blocked, which implied that, during the PI-1840-induced cycle arrest, the accumulation of p27 and its restriction on G_1-S transition exerted a less pronounced effect on cell cycle arrest compared with the overexpression of G_2/M checkpoint restrictors.

An aberrant activation of the NF-κB pathway is common in a variety of types of human cancer, and this also holds true for OS cells (21). A previous study demonstrated that proteasome inhibitors may inhibit the NF-κB pathway in intrahepatic cholangiocarcinoma (22), and the NF-κB pathway is one of the upstream pathways of apoptosis (23). In the present study, it was confirmed that PI-1840 could suppress the NF-κB pathway, and subsequently induce OS cells to apoptosis in a caspase-dependent manner. It was revealed that, in PI-1840-induced apoptosis, the NF-κB pathway was an important activatory factor, but not the only one, as determined by the findings of the downregulation of cleaved caspase-3 and the increased cell viability, partly after application of IκBα siRNA. Several key proteins lying further downstream in the apoptosis signaling pathway were also investigated. The level of Bcl-2, an anti-apoptotic protein that promotes cell survival in response to a wide range of apoptotic stimuli through inhibition of mitochondrial Cyto *c* release (24), decreased as the concentration of PI-1840 was increased. Furthermore, the level of Cyto *c* in mitochondria decreased, which confirmed the presence of apoptosis of the OS cells at the mitochondrial level (25). In addition, the enhanced expression of cleaved caspase-8 and cleaved caspase-9 suggested that the PI-1840-induced apoptosis was associated with the intrinsic and the extrinsic apoptotic pathways (26,27).

Previous studies have revealed that proteasome inhibitors are able to inhibit the metastasis of tumor cells *in vitro* and *in vivo* (28,29), although none of the tested proteasome inhibitors were non-covalent. The aforementioned results revealed that PI-1840 suppresses the NF-κB pathway, and that inhibiting the NF-κB pathway may suppress the metastasis capability of the tumor cells (30-32). In the present study, using western blot

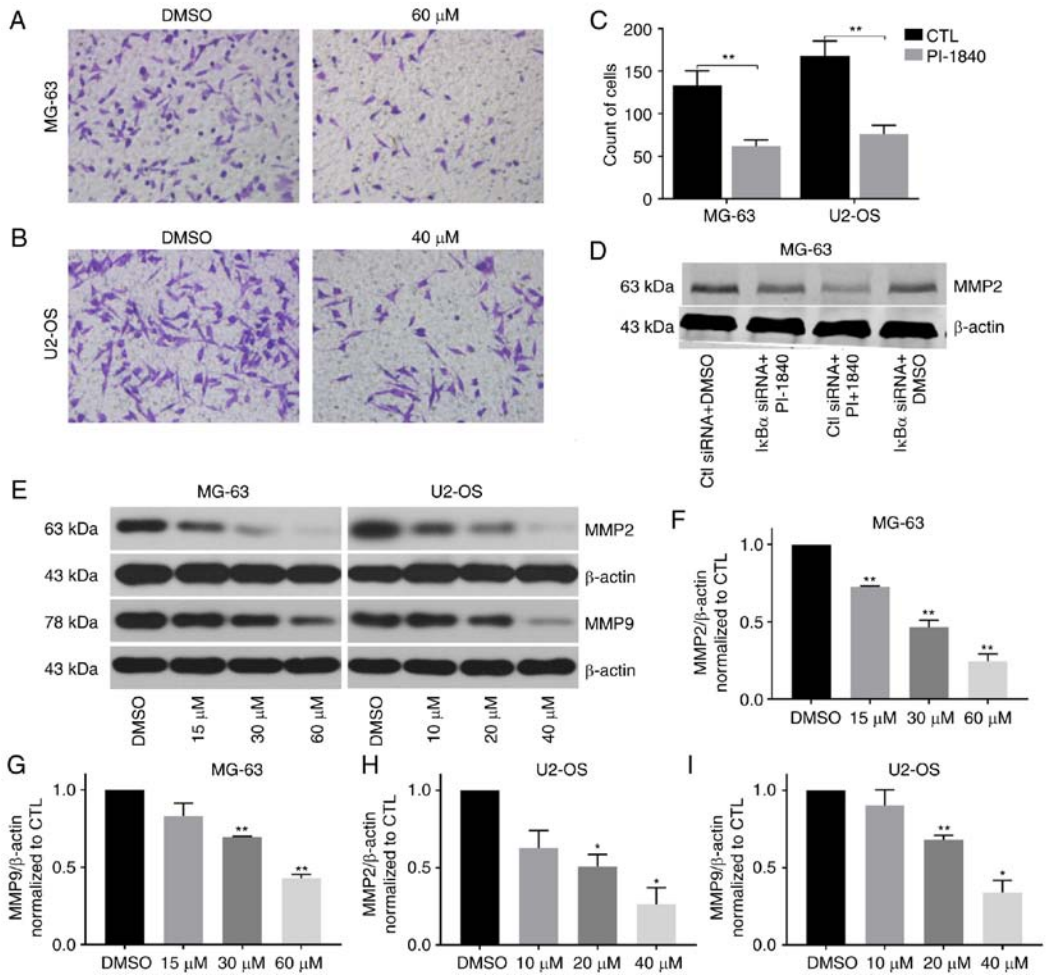

Figure 10. (A-C) In Transwell assays, following exposure to PI-1840 for 48 h, the cell count in the lower chamber was significantly decreased (magnification, x200; n=4). **P<0.01 compared with the DMSO group. (D) Following pretreatment of the cells with IκBα siRNA, and subsequent treatment with PI-1840 (60 μM) for 48 h, the expression level of MMP2 was increased compared with the group co-treated with PI-1840 (60 μM) and control siRNA. (E-I) The protein levels of MMP2 and MMP9 decreased with increasing concentrations of PI-1840 (48 h) (n=3). *P<0.05; **P<0.01 compared with the DMSO group. CTL, control; DMSO, dimethyl sulfoxide; MMP, matrix metalloproteinase.

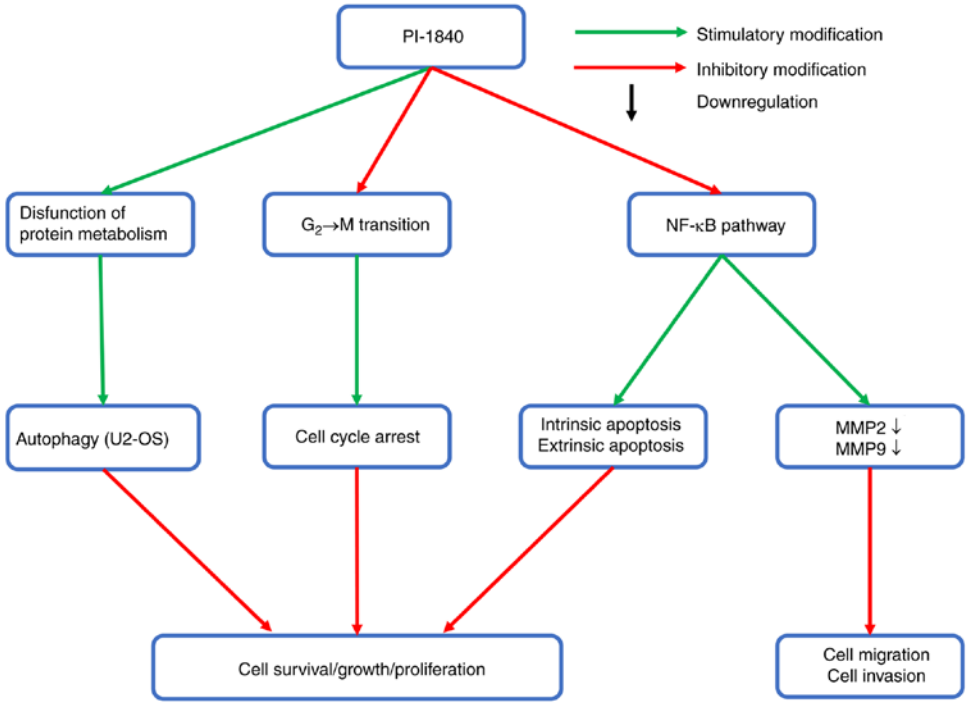

Figure 11. Schematic diagram of the potential molecular mechanisms associated with the anticancer effects of PI-1840.

analysis and Transwell assay, it was confirmed that PI-1840 was able to attenuate the metastatic ability of the OS cells through inhibition of the NF-κB pathway and downregulation of the expression level of MMPs.

Unlike apoptosis, the role of autophagy in cell death and antitumor function remains controversial (33-35). Autophagy may increase the survival rate of cells when they are confronted with starvation, toxic substances or infection (36,37). In contrast, autophagy is detrimental to cells under certain circumstances, particularly tumor cells (38,39). Furthermore, a complex situation exists between metabolic disorders of proteins and autophagy (40), and PI-1840 may disturb protein metabolism. Hence, in the present study, the autophagic response of OS cells was investigated by western blot analysis and mRFP-GFP-LC3 adenovirus assay. Beclin1, a protein whose levels are positively associated with the level of autophagy, was overexpressed in the two cell lines in a dose-dependent manner following treatment with PI-1840, and knowledge of its anticancer activity has been emerging in recent years (41). To inhibit autophagy of the OS cells, chloroquine was used, and subsequently a CCK-8 assay was performed to determine whether the PI-1840-induced autophagy could influence the survival rate. Our results indicated that, in the MG-63 cell line, autophagy did not affect the survival rate of OS cells, and these results were consistent with a previous study published by our group (18). However, in the U2-OS cell line, the inhibition of autophagy enhanced the survival rate of cells, which implied that the function of PI-1840-induced autophagy is dependent on the type of cell under consideration.

In conclusion, the present study has systematically demonstrated the anticancer activity of a non-covalent proteasome inhibitor, PI-1840, in the OS cell lines, MG-63 and U2-OS, by means of inhibiting proliferation and metastasis, and inducing cell cycle arrest, apoptosis and autophagy. A schematic representation of these findings is presented in Fig. 11. These results provide a foundation for PI-1840 to become a potential antitumor agent in OS treatment. However, further studies are required to analyze the complex cross-talk that exists among the NF-κB, apoptosis and autophagy signaling pathways (42,43). A further limitation was that we were unable to conduct assays to observe changes in tumor weight and metastasis *in vivo* after treatment with PI-1840 in an experimental animal model, due to a lack of available funds. Furthermore, in view of its different anticancer mechanism with respect to the already employed drugs for OS treatment, it would be interesting to explore the effects of PI-1840 in combination with other first-line drugs, such as doxorubicin or cisplatin, on OS.

Acknowledgements

The authors are grateful to staff from the High-Tech Zone Laboratory of Public Test and Analysis Service (Shenyang, China) for their assistance in these experiments.

Funding

Training funds for doctoral students were provided by The First Affiliated Hospital of Harbin Medical University.

Availability of data and materials

The datasets used during the present study are available from the corresponding author upon reasonable request.

Authors' contributions

ZB and YC conceived and designed the experiments. YC, HX, HC, SY and CG performed the experiments. YC, HC, HX, SY and LY analyzed the data. ZB and YC wrote the manuscript. All authors read and approved the final manuscript and agree to be accountable for all aspects of the research in ensuring that the accuracy or integrity of any part of the work are appropriately investigated and resolved.

Ethics approval and consent to participate

Not applicable.

Patient consent for publication

Not applicable.

Competing interests

The authors declare that they have no competing interests.

References

1. Bielack SS, Kempf-Bielack B, Delling G, Exner GU, Flege S, Helmke K, Kotz R, Salzer-Kuntschik M, Werner M, Winkelmann W, *et al*: Prognostic factors in high-grade osteosarcoma of the extremities or trunk: An analysis of 1,702 patients treated on neoadjuvant cooperative osteosarcoma study group protocols. J Clin Oncol 20: 776-790, 2002.
2. Harrison DJ, Geller DS, Gill JD, Lewis VO and Gorlick R: Current and future therapeutic approaches for osteosarcoma. Expert Rev Anticancer Ther 18: 39-50, 2018.
3. Isakoff MS, Bielack SS, Meltzer P and Gorlick R: Osteosarcoma: Current treatment and a collaborative pathway to success. J Clin Oncol 33: 3029-3035, 2015.
4. Smith MA, Seibel NL, Altekruse SF, Ries LA, Melbert DL, O'Leary M, Smith FO and Reaman GH: Outcomes for children and adolescents with cancer: Challenges for the twenty-first century. J Clin Oncol 28: 2625-2634, 2010.
5. Yamamoto N and Tsuchiya H: Chemotherapy for osteosarcoma-where does it come from? What is it? Where is it going? Expert Opin Pharmacother 14: 2183-2193, 2013.
6. Chen L and Madura K: Increased proteasome activity, ubiquitin-conjugating enzymes, and eEF1A translation factor detected in breast cancer tissue. Cancer Res 65: 5599-5606, 2005.
7. Cenci S, Oliva L, Cerruti F, Milan E, Bianchi G, Raule M, Mezghrani A, Pasqualetto E, Sitia R and Cascio P: Pivotal advance: Protein synthesis modulates responsiveness of differentiating and malignant plasma cells to proteasome inhibitors. J Leukoc Biol 92: 921-931, 2012.
8. Voutsadakis IA: Proteasome expression and activity in cancer and cancer stem cells. Tumor Biol 39: 1010428317692248, 2017.
9. Teicher BA and Tomaszewski JE: Proteasome inhibitors. Biochem Pharmacol 96: 1-9, 2015.
10. Moreau P, Masszi T, Grzasko N, Bahlis NJ, Hansson M, Pour L, Sandhu I, Ganly P, Baker BW, Jackson SR, *et al*: Oral ixazomib, lenalidomide, and dexamethasone for multiple myeloma. N Engl J Med 374: 1621-1634, 2016.
11. Palumbo A, Chanan-Khan A, Weisel K, Nooka AK, Masszi T, Beksac M, Spicka I, Hungria V, Munder M, Mateos MV, *et al*: Daratumumab, bortezomib, and dexamethasone for multiple myeloma. N Engl J Med 375: 754-766, 2016.
12. McBride A, Klaus JO and Stockerl-Goldstein K: Carfilzomib: A second-generation proteasome inhibitor for the treatment of multiple myeloma. Am J Heal Pharm 72: 353-360, 2015.

13. Lou Z, Ren T, Peng X, Sun Y, Jiao G, Lu Q, Zhang S, Lu X and Guo W: Bortezomib induces apoptosis and autophagy in osteosarcoma cells through mitogen-activated protein kinase pathway in vitro. J Int Med Res 41: 1505-1519, 2013.
14. Liu R, Fu C, Sun J, Wang X, Geng S, Wang X, Zou J, Bi Z and Yang C: A new perspective for osteosarcoma therapy: Proteasome inhibition by MLN9708/2238 successfully induces apoptosis and cell cycle arrest and attenuates the invasion ability of osteosarcoma cells in vitro. Cell Physiol Biochem 41: 451-465, 2017.
15. Singh J, Petter RC, Baillie TA and Whitty A: The resurgence of covalent drugs. Nat Rev Drug Discov 10: 307-317, 2011.
16. Ozcan S, Kazi A, Marsilio F, Fang B, Guida WC, Koomen J, Lawrence HR and Sebti SM: Oxadiazole-isopropylamides as potent and noncovalent proteasome inhibitors. J Med Chem 56: 3783-3805, 2013.
17. Kazi A, Ozcan S, Tecleab A, Sun Y, Lawrence HR and Sebti SM: Discovery of PI-1840, a novel noncovalent and rapidly reversible proteasome inhibitor with anti-tumor activity. J Biol Chem 289: 11906-11915, 2014.
18. Zou J, Zhang Y, Sun J, Wang X, Tu H, Geng S, Liu R, Chen Y and Bi Z: Deoxyelephantopin induces reactive oxygen species-mediated apoptosis and autophagy in human osteosarcoma cells. Cell Physiol Biochem 42: 1812-1821, 2017.
19. Gu JJ, Hernandez-Ilizaliturri FJ, Kaufman GP, Czuczman NM, Mavis C, Skitzki JJ and Czuczman MS: The novel proteasome inhibitor carfilzomib induces cell cycle arrest, apoptosis and potentiates the anti-tumour activity of chemotherapy in rituximab-resistant lymphoma. Br J Haematol 162: 657-669, 2013.
20. Choi YH and Yoo YH: Taxol-induced growth arrest and apoptosis is associated with the upregulation of the Cdk inhibitor, $p21^{WAF1/CIP1}$, in human breast cancer cells. Oncol Rep 28: 2163-2169, 2012.
21. Di W, Khan M, Rasul A, Sun M, Sui Y, Zhong L, Yang L, Zhu Q, Feng L and Ma T: Isoalantolactone inhibits constitutive NF-κB activation and induces reactive oxygen species-mediated apoptosis in osteosarcoma U2OS cells through mitochondrial dysfunction. Oncol Rep 32: 1585-1593, 2014.
22. Yu GY, Wang X, Zheng SS, Gao XM, Jia QA, Zhu WW, Lu L, Jia HL, Chen JH, Dong QZ, *et al*: RA190, a proteasome subunit ADRM1 inhibitor, suppresses intrahepatic cholangiocarcinoma by inducing NF-κB-mediated cell apoptosis. Cell Physiol Biochem 47: 1152-1166, 2018.
23. Zhang CL, Wang C, Yan WJ, Gao R, Li YH and Zhou XH: Knockdown of TNFAIP1 inhibits growth and induces apoptosis in osteosarcoma cells through inhibition of the nuclear factor-κB pathway. Oncol Rep 32: 1149-1155, 2014.
24. Murphy KM, Ranganathan V, Farnsworth ML, Kavallaris M and Lock RB: Bcl-2 inhibits Bax translocation from cytosol to mitochondria during drug-induced apoptosis of human tumor cells. Cell Death Differ 7: 102-111, 2000.
25. Zhu Y, Li M, Wang X, Jin H, Liu S, Xu J and Chen Q: Caspase cleavage of cytochrome *c*1 disrupts mitochondrial function and enhances cytochrome *c* release. Cell Res 22: 127-141, 2012.
26. Djiadeu P, Farmakovski N, Azzouz D, Kotra LP, Sweezey N and Palaniyar N: Surfactant protein D regulates caspase-8-mediated cascade of the intrinsic pathway of apoptosis while promoting bleb formation. Mol Immunol 92: 190-198, 2017.
27. Aral K, Aral CA and Kapila Y: The role of caspase-8, caspase-9, and apoptosis inducing factor in periodontal disease. J Periodontol 90: 288-294, 2019.
28. Chauhan D, Tian Z, Zhou B, Kuhn D, Orlowski R, Raje N, Richardson P and Anderson KC: In vitro and in vivo selective antitumor activity of a novel orally bioavailable proteasome inhibitor MLN9708 against multiple myeloma cells. Clin Cancer Res 17: 5311-5321, 2011.
29. Bao X, Ren T, Huang Y, Ren C, Yang K, Zhang H and Guo W: Bortezomib induces apoptosis and suppresses cell growth and metastasis by inactivation of Stat3 signaling in chondrosarcoma. Int J Oncol 50: 477-486, 2017.
30. Yin X, Feng C, Han L, Ma Y, Jiao Y, Wang J, Jia L, Jing F, Gao X, Zhang Y, *et al*: Diallyl disulfide inhibits the metastasis of type II esophageal-gastric junction adenocarcinoma cells via NF-κB and PI3K/AKT signaling pathways *in vitro*. Oncol Rep 39: 784-794, 2018.
31. Liao D, Zhong L, Duan T, Zhang RH, Wang X, Wang G, Hu K, Lv X and Kang T: Aspirin suppresses the growth and metastasis of osteosarcoma through the NF-κB pathway. Clin Cancer Res 21: 5349-5359, 2015.
32. Jiang Q, Pan Y, Cheng Y, Li H, Liu D and Li H: Lunasin suppresses the migration and invasion of breast cancer cells by inhibiting matrix metalloproteinase-2/-9 via the FAK/Akt/ERK and NF-κB signaling pathways. Oncol Rep 36: 253-262, 2016.
33. Zhang H: Targeting autophagy in lymphomas: A double-edged sword? Int J Hematol 107: 502-512, 2018.
34. Mehrpour M, Esclatine A, Beau I and Codogno P: Autophagy in health and disease. 1. Regulation and significance of autophagy: An overview. Am J Physiol Cell Physiol 298: C776-C785, 2010.
35. Gewirtz DA: The four faces of autophagy: Implications for cancer therapy. Cancer Res 74: 647-651, 2014.
36. Karsli-Uzunbas G, Guo JY, Price S, Teng X, Laddha SV, Khor S, Kalaany NY, Jacks T, Chan CS, Rabinowitz JD and White E: Autophagy is required for glucose homeostasis and lung tumor maintenance. Cancer Discov 4: 914-927, 2014.
37. Bronietzki AW, Schuster M and Schmitz I: Autophagy in T-cell development, activation and differentiation. Immunol Cell Biol 93: 25-34, 2015.
38. Wu J, Gao F, Xu T, Deng X, Wang C, Yang X, Hu Z, Long Y, He X, Liang G, *et al*: miR-503 suppresses the proliferation and metastasis of esophageal squamous cell carcinoma by triggering autophagy via PKA/mTOR signaling. Int J Oncol: Mar 16, 2018 (Epub ahead of print).
39. Zhao H, Jia H, Han Q and Zhang J: Homeobox containing 1 inhibits liver cancer progression by promoting autophagy as well as inhibiting stemness and immune escape. Oncol Rep 40: 1657-1665, 2018.
40. White E, Mehnert JM and Chan CS: Autophagy, metabolism, and cancer. Clin Cancer Res 21: 5037-5046, 2015.
41. Zhu J, Cai Y, Xu K, Ren X, Sun J, Lu S, Chen J and Xu P: Beclin1 overexpression suppresses tumor cell proliferation and survival via an autophagy-dependent pathway in human synovial sarcoma cells. Oncol Rep 40: 1927-1936, 2018.
42. Su J, Liu F, Xia M, Xu Y, Li X, Kang J, Li Y and Sun L: p62 participates in the inhibition of NF-κB signaling and apoptosis induced by sulfasalazine in human glioma U251 cells. Oncol Rep 34: 235-243, 2015.
43. Qian HR, Shi ZQ, Zhu HP, Gu LH, Wang XF and Yang Y: Interplay between apoptosis and autophagy in colorectal cancer. Oncotarget 8: 62759-62768, 2017.